2.3 Modal decomposition

2.3.1 Structure without rigid body modes

Let us perform a change of variables from physical coordinates x to modal coordinates according to

$$x = \Phi z \tag{2.10}$$

where z is the vector of modal amplitudes. Substituting into Equ.(2.2), we get

$$M\Phi\ddot{z} + C\Phi\dot{z} + K\Phi z = f$$

Left multiplying by Φ^T and using the orthogonality relationships (2.8) and (2.9), we obtain

$$diag(\mu_i)\ddot{z} + \Phi^T C\Phi\dot{z} + diag(\mu_i\omega_i^2)z = \Phi^T f \tag{2.11}$$

If the matrix $\Phi^T C\Phi$ is diagonal, the damping is said *classical* or *normal*. In this case, the modal fraction of critical damping ξ_i (in short modal damping) is defined by

$$\Phi^T C\Phi = diag(2\xi_i\mu_i\omega_i) \tag{2.12}$$

One can readily check that the Rayleigh damping (2.3) complies with this condition and that the corresponding modal damping ratios are

$$\xi_i = \frac{1}{2}(\frac{\alpha}{\omega_i} + \beta\omega_i) \tag{2.13}$$

The two free parameters α and β can be selected in order to match the modal damping of two modes. Note that the Rayleigh damping tends to overestimate the damping of the high frequency modes.

Under condition (2.12), the modal equations are decoupled and Equ.(2.11) can be rewritten

$$\ddot{z} + 2\xi\Omega\,\dot{z} + \Omega^2 z = \mu^{-1}\Phi^T f \tag{2.14}$$

with the notations

$$\begin{aligned} \xi &= diag(\xi_i) \\ \Omega &= diag(\omega_i) \\ \mu &= diag(\mu_i) \end{aligned} \tag{2.15}$$

The following values of the modal damping ratio can be regarded as typical: satellites and space structures are generally very lightly damped ($\xi \simeq 0.001 - 0.005$), because of the extensive use of fiber reinforced composites, the absence of aerodynamic damping, and the low strain level. Mechanical engineering applications (steel structures, piping,...) are in the range of $\xi \simeq 0.01 - 0.02$; most dissipation takes place in the joints, and the damping increases with the strain level. For civil engineering applications, $\xi \simeq 0.05$ is typical and, when radiation damping through the ground is involved, it may reach $\xi \simeq 0.20$, depending on the local soil conditions. The assumption of classical damping is often justified for light damping, but it is questionable when the damping is large, as in problems involving soil-structure interaction. Lightly damped structures are usually easier to model, but more difficult to control, because their poles are located very near the imaginary axis and they can be destabilized very easily.

If one accepts the assumption of classical damping, the only difference between Equ.(2.2) and (2.14) lies in the change of coordinates (2.10). However, in physical coordinates, the number of degrees of freedom of a discretized model of the form (2.2) is usually large, especially if the geometry is complicated, because of the difficulty of accurately representing the stiffness of the structure. This number of degrees of freedom is unnecessarily large to represent the structural response in a limited bandwidth. If a structure is excited by a band-limited excitation, its response is dominated by the normal modes whose natural frequencies belong to the bandwidth of the excitation, and the integration of Equ.(2.14) can often be restricted to these modes. The number of degrees of freedom contributing effectively to the response is therefore reduced drastically in modal coordinates.

Now, let us consider the steady state response to a harmonic excitation $f = Fe^{j\omega t}$. The response will also be harmonic with the same frequency, $x = Xe^{j\omega t}$; substituting into Equ.(2.2), we find that the complex amplitudes of F and X are related by

$$X = [-\omega^2 M + j\omega C + K]^{-1} F = G(\omega) F \tag{2.16}$$

The matrix $G(\omega)$ is the dynamic generalization of the flexibility matrix K^{-1} and is called the *dynamic flexibility matrix*. Equ.(2.16) can be obtained alternatively by Fourier transformation of Equ.(2.2).

If one considers the same problem in modal coordinates, the modal amplitudes will also be harmonic, $z = Ze^{j\omega t}$ and, from Equ.(2.14), we obtain

$$Z = diag\{\frac{1}{\mu_i(\omega_i^2 - \omega^2 + 2j\xi_i\omega_i\omega)}\}\Phi^T F \tag{2.17}$$

From Equ.(2.10),

$$X = \Phi Z = \Phi diag\{\frac{1}{\mu_i(\omega_i^2 - \omega^2 + 2j\xi_i\omega_i\omega)}\}\Phi^T F \tag{2.18}$$

Comparing Equ.(2.16) and (2.18), we obtain the modal expansion of the dynamic flexibility matrix:

$$G(\omega) = [-\omega^2 M + j\omega C + K]^{-1} = \sum_{i=1}^{n} \frac{\phi_i \phi_i^T}{\mu_i(\omega_i^2 - \omega^2 + 2j\xi_i\omega_i\omega)} \tag{2.19}$$

where the sum extends to all the modes. $G_{lk}(\omega)$ expresses the complex amplitude of the structural response of degree of freedom l when the structure is exposed to a steady state harmonic excitation $e^{j\omega t}$ at degree of freedom k. If the structure has no rigid body modes, we can write Equ.(2.19) for $\omega = 0$; we obtain the modal expansion of the static flexibility matrix:

$$G(0) = K^{-1} = \sum_{i=1}^{n} \frac{\phi_i \phi_i^T}{\mu_i \omega_i^2} = \Phi(\Phi^T K \Phi)^{-1} \Phi^T \tag{2.20}$$

For a limited frequency band $\omega < \omega_b$, if we select m in such a way that $\omega_b \ll \omega_m$, the dynamic expansion can be split into the contribution of the low frequency modes ($i \leq m$) which respond dynamically, and that of the high frequency modes which respond statically:

$$G(\omega) \simeq \sum_{i=1}^{m} \frac{\phi_i \phi_i^T}{\mu_i(\omega_i^2 - \omega^2 + 2j\xi_i\omega_i\omega)} + \sum_{i=m+1}^{n} \frac{\phi_i \phi_i^T}{\mu_i \omega_i^2} \tag{2.21}$$

Using Equ.(2.20), we can transform the foregoing result in such a way that the high frequency modes do not appear explicitly in the expansion:

$$G(\omega) \simeq \sum_{i=1}^{m} \frac{\phi_i \phi_i^T}{\mu_i(\omega_i^2 - \omega^2 + 2j\xi_i\omega_i\omega)} + K^{-1} - \sum_{i=1}^{m} \frac{\phi_i \phi_i^T}{\mu_i \omega_i^2} \tag{2.22}$$

The static contribution of the high frequency modes to the flexibility matrix is often called the *residual mode*; we shall denote it R. It is independent of the frequency ω and introduces a *feedthrough* component in the transfer matrix: part of the output is proportional to the input. In terms of Laplace transform, the numerator and the denominator of some components of $G(s)$ have the same power in s (such a transfer function is said to be *not strictly proper*). We shall see later that truncating the modal expansion of a transfer function without introducing a residual mode can lead to substantial errors in the prediction of the open-loop zeros (e.g. see Fig.3.15) and, as a result, of the performance of a control system.

2.3.2 Structure with rigid body modes

The approximation (2.22) applies only at low frequency, $\omega < \omega_m$. If the structure has r rigid body modes, the first sum can be split into rigid and flexible modes; however, the residual mode cannot be used any more, because K^{-1} no longer exists. This problem can be solved in the following way. The displacements are partitioned into their rigid and flexible contributions according to

$$x = x_r + x_e = \Phi_r z_r + \Phi_e z_e \tag{2.23}$$

where Φ_r and Φ_e are the matrices whose columns are the rigid body modes and the flexible modes, respectively. Assuming no damping, to make things formally or

$$P = \frac{1}{3}\begin{pmatrix} 2 & -1 & -1 \\ -1 & 2 & -1 \\ -1 & -1 & 2 \end{pmatrix}$$

We can readily check that

$$P\Phi = P(\Phi_r, \Phi_e) = (0, \Phi_e)$$

and the self-equilibrated loads associated with a force f applied to mass 1 is (Fig.2.3.a)

$$P^T f = \frac{1}{3}\begin{pmatrix} 2 & -1 & -1 \\ -1 & 2 & -1 \\ -1 & -1 & 2 \end{pmatrix}\begin{pmatrix} f \\ 0 \\ 0 \end{pmatrix} = \begin{pmatrix} 2/3 \\ -1/3 \\ -1/3 \end{pmatrix} f$$

If we impose the statically determinate constraint on mass 1 (Fig.2.3.b), the resulting flexibility matrix is

$$G_{iso} = \frac{1}{k}\begin{pmatrix} 0 & 0 & 0 \\ 0 & 1 & 1 \\ 0 & 1 & 2 \end{pmatrix}$$

leading to

$$PG_{iso}P^T = \frac{1}{9k}\begin{pmatrix} 5 & -1 & -4 \\ -1 & 2 & -1 \\ -4 & -1 & 5 \end{pmatrix}$$

The reader can easily check that other dummy constraints would lead to the same pseudo-static flexibility matrix (Problem P.2.3).

2.4 Transfer function of collocated systems

Consider a diagonal component of the dynamic flexibility matrix of a undamped system. It is the transfer function between the generalized force (point force or torque) and the response of the corresponding degree of freedom (respectively displacement or angle). If the force is generated by an actuator, and the displacement is measured by a sensor, the actuator and sensor are *collocated*. We shall see later that control systems using collocated actuator/sensor pairs usually enjoy special properties which are the consequence of alternating poles and zeros along the imaginary axis. To establish this property, consider the k^{th} diagonal term of Equ.(2.34):

$$G_{kk}(\omega) = \sum_{i=1}^{r} \frac{\phi_i^2(k)}{-\mu_i\omega^2} + \sum_{i=r+1}^{m} \frac{\phi_i^2(k)}{\mu_i(\omega_i^2 - \omega^2)} + R_{kk} \qquad (2.36)$$

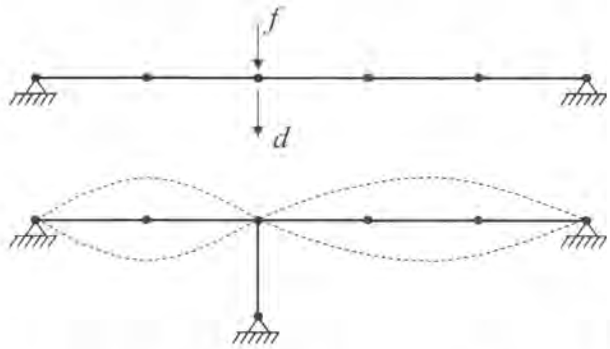

Figure 2.4: *(a) Structure with collocated actuator and sensor. (b) Mode shape of the structure with additional restraint.*

$G_{kk}(\omega)$ is real since the system is undamped, and all the numerators in the modal expansion are positive. As a result, it is readily demonstrated that

$$\frac{\mathrm{d}G_{kk}(\omega^2)}{\mathrm{d}\omega^2} \geq 0 \tag{2.37}$$

The behaviour of $G_{kk}(\omega)$ is represented in Fig.2.5: The amplitude of the transfer function goes to $\pm\infty$ at the resonance frequencies ω_i (corresponding to a pair of purely imaginary poles in the system). In every interval between consecutive resonance frequencies, there is a frequency ω_{0_j} where the amplitude of the frequency response function (FRF) vanishes; in structural dynamics, these frequencies are called *anti-resonance* frequencies; they correspond to purely imaginary transmission zeros in the open-loop transfer function $G_{kk}(s)$. It is worth mentioning that

- A harmonic excitation at an anti-resonance frequency produces no response at the degree of freedom where the excitation is applied; the structure behaves as if an additional restraint had been added. The anti-resonance frequencies are in fact identical to the resonance frequencies of the system with the additional restraint (Fig.2.4), and the acting force is identical to the reaction force in the additional restraint during the free vibration of the modified system.

- In contrast to the resonance frequencies, the anti-resonance frequencies do depend on the actuator location. If the diagram $G_{ll}(\omega)$ of another diagonal component is examined, the frequencies where the plot goes to $\pm\infty$ (resonances) are unchanged, but the frequencies where $G_{ll}(\omega) = 0$ do change (as do the natural frequencies of the modified system when we change the location of the additional restraint). In all cases, however, there will be one and only one anti-resonance between two consecutive resonances.

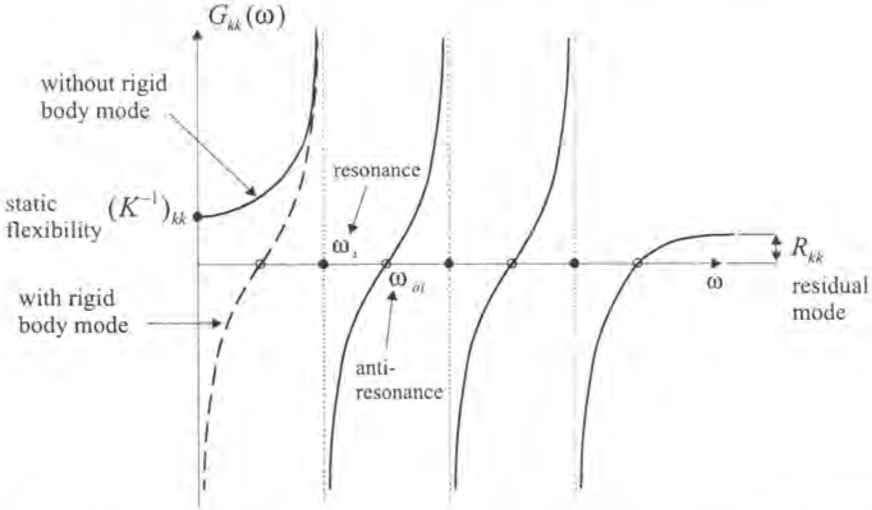

Figure 2.5: *FRF of a undamped structure with collocated actuator and sensor.*

- Observing Fig.2.5 and Equ.(2.36), we see that neglecting the residual mode R_{kk} is equivalent to moving the *FRF* $G_{kk}(\omega)$ downwards by R_{kk}. Doing that, all the anti-resonance frequencies tend to be overestimated by an amount which depends on the slope of $G_{kk}(\omega)$ in the vicinity of the zeros. We shall see later that errors in the spacing between poles and zeros of the open-loop system can lead to substantial errors in the performance of the closed-loop system.

- For a system with non-collocated actuator and sensor, the numerators of the various terms in the modal expansion of $G_{kl}(\omega)$ become $\phi_i(k)\phi_i(l)$; they can be either positive or negative, and the property (2.37) is lost. Interlacing poles and zeros are no longer guaranteed in this case.

In system theory, it is customary to write the system transfer functions in the form

$$G(s) = k\,\frac{\prod_{\text{zeros}}(s - z_i)}{\prod_{\text{poles}}(s - p_i)} \tag{2.38}$$

In the present case, the undamped collocated system has alternating imaginary poles and zeros at $p_i = \pm j\omega_i$ and $z_i = \pm j\omega_{0i}$ (Fig.2.6.a). The transfer function reads

$$G(s) = k\,\frac{\prod_{\text{zeros}}(s^2 + \omega_{0i}^2)}{\prod_{\text{poles}}(s^2 + \omega_i^2)} \tag{2.39}$$

If some damping is added, the poles and zeros are slightly moved into the left half plane as indicated in Fig.2.6.b, without changing the dominant feature of

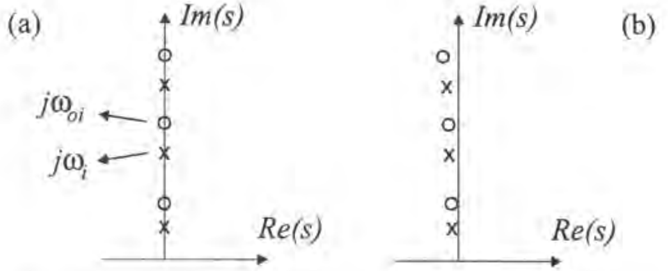

Figure 2.6: *Pole/zero pattern of a structure with collocated actuator and sensor. (a) Undamped. (b) Lightly damped. (Only the upper half of the complex plane is shown, the diagram is symmetrical with respect to the real axis).*

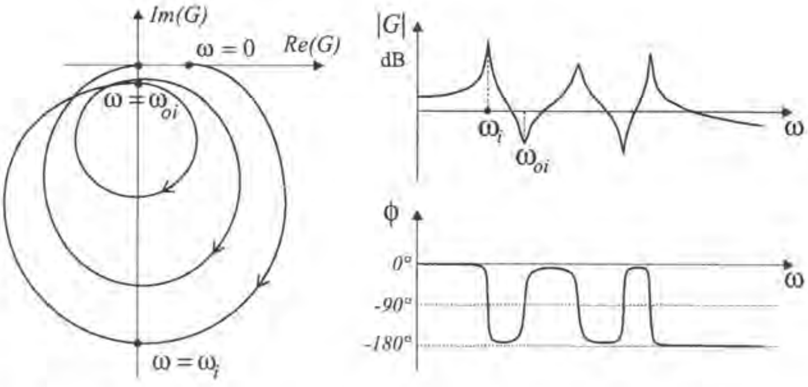

Figure 2.7: *Nyquist diagram and Bode plots of a lightly damped structure with collocated actuator and sensor.*

interlacing. A collocated system always exhibits Bode and Nyquist plots similar to those represented in Fig.2.7. Each flexible mode introduces a circle in the Nyquist diagram; it is more or less centered on the imaginary axis which is intersected at $\omega = \omega_i$ and $\omega = \omega_{0i}$; the radius is proportional to the inverse of the modal damping, ξ_i^{-1}. In the Bode plots, a 180^0 phase lag occurs at every natural frequency, and is compensated by a 180^0 phase lead at every imaginary zero; the phase always oscillates between 0 and $-\pi$, as a result of the interlacing property of the poles and zeros.

2.5 Continuous structures

Continuous structures are distributed parameter systems which are governed by partial differential equations. Various discretization techniques, such as the Rayleigh-Ritz method, or finite elements, allow us to approximate the partial differential equation by a finite set of ordinary differential equations. In this section, we illustrate some of the features of distributed parameter systems with continuous beams. This example will be frequently used in the subsequent chapters.

The plane transverse vibration of a beam is governed by the following partial differential equation

$$(EIw'')'' + m\ddot{w} = p \tag{2.40}$$

This equation is based on the Euler-Bernouilli assumptions that the neutral axis undergoes no extension and that the cross section remains perpendicular to the neutral axis (no shear deformation). EI is the bending stiffness, m is the mass per unit length and p the distributed external load per unit length. If the beam is uniform, the free vibration is governed by

$$w^{IV} + \frac{m}{EI}\ddot{w} = 0 \tag{2.41}$$

The boundary conditions depend on the support configuration: a simple support implies $w = 0$ and $w'' = 0$ (no displacement, no bending moment); for a clamped end, we have $w = 0$ and $w' = 0$ (no displacement, no rotation); a free end corresponds to $w'' = 0$ and $w''' = 0$ (no bending moment, no shear), etc...

A harmonic solution of the form $w(x,t) = \phi(x)\,e^{j\omega t}$ can be obtained if $\phi(x)$ and ω satisfy

$$\frac{d^4\phi}{dx^4} - \frac{m}{EI}\omega^2\phi = 0 \tag{2.42}$$

with the appropriate boundary conditions. This equation defines a eigenvalue problem; the solution consists of the natural frequencies ω_i (infinite in number) and the corresponding mode shapes $\phi_i(x)$. The eigenvalues are tabulated for various boundary conditions in textbooks on mechanical vibrations (e.g. Geradin & Rixen, p.187). For the pinned-pinned case, the natural frequencies and mode shapes are

$$\omega_n^2 = (n\pi)^4\frac{EI}{ml^4} \tag{2.43}$$

$$\phi_n(x) = \sin\frac{n\pi x}{l} \tag{2.44}$$

Just as for discrete systems, the mode shapes are orthogonal with respect to the mass and stiffness distribution:

$$\int_0^l m\,\phi_i(x)\phi_j(x)\,dx = \mu_i\delta_{ij} \tag{2.45}$$

$$\int_0^l EI\,\phi_i''(x)\phi_j''(x)\,dx = \mu_i\omega_i^2\delta_{ij} \tag{2.46}$$

The generalized mass corresponding to Equ.(2.44) is $\mu_n = ml/2$. As with discrete structures, the frequency response function between a point force actuator at x_a and a displacement sensor at x_s is

$$G(\omega) = \sum_{i=1}^{\infty} \frac{\phi_i(x_a)\phi_i(x_s)}{\mu_i(\omega_i^2 - \omega^2 + 2j\xi_i\omega_i\omega)} \tag{2.47}$$

where the sum extends to infinity. Exactly as for discrete systems, the expansion can be limited to a finite set of modes, the high frequency modes being included in a quasi-static correction as in Equ.(2.34) (Problem P.2.5).

2.6 Guyan reduction

As already mentioned, the size of a discretized model obtained by finite elements is essentially governed by the representation of the stiffness of the structure. For complicated geometries, it may become very large, especially with automated mesh generators. Before solving the eigenvalue problem (2.5), it may be advisable to reduce the size of the model (2.2) by condensing the degrees of freedom with little or no inertia and which are not excited by external forces. The degrees of freedom to be condensed, denoted x_2 in what follows, are often referred to as *slaves*; those kept in the reduced model are called *masters* and are denoted x_1.

To begin with, consider the undamped forced vibration of a structure where the slaves x_2 are not excited and have no inertia; the governing equation is

$$\begin{pmatrix} M_{11} & 0 \\ 0 & 0 \end{pmatrix}\begin{pmatrix} \ddot{x}_1 \\ \ddot{x}_2 \end{pmatrix} + \begin{pmatrix} K_{11} & K_{12} \\ K_{21} & K_{22} \end{pmatrix}\begin{pmatrix} x_1 \\ x_2 \end{pmatrix} = \begin{pmatrix} f_1 \\ 0 \end{pmatrix} \tag{2.48}$$

or

$$M_{11}\ddot{x}_1 + K_{11}x_1 + K_{12}x_2 = f_1 \tag{2.49}$$

$$K_{21}x_1 + K_{22}x_2 = 0 \tag{2.50}$$

According to the second equation, the slaves x_2 are completely determined by the masters x_1:

$$x_2 = -K_{22}^{-1}K_{21}x_1 \tag{2.51}$$

Substituting into Equ.(2.49), we find the reduced equation

$$M_{11}\ddot{x}_1 + (K_{11} - K_{12}K_{22}^{-1}K_{21})x_1 = f_1 \tag{2.52}$$

which involves only x_1. Note that in this case, the reduced equation has been obtained without approximation.

Chapter 4

Collocated versus non-collocated control

4.1 Introduction

In the foregoing chapters, we have seen that the use of collocated actuator and sensor pairs, for a lightly damped flexible structure, always leads to alternating poles and zeros near the imaginary axis (Fig.4.1.a). In this chapter, using the root locus technique, we show that this property guarantees the asymptotic stability of a wide class of single-input single-output (*SISO*) control systems, even if the system parameters are subject to large perturbations. This is because the root locus plot keeps the same general shape, and remains entirely within the left half plane when the system parameters are changed from their nominal values. Such a control system is said to be *robust* with respect to stability. The

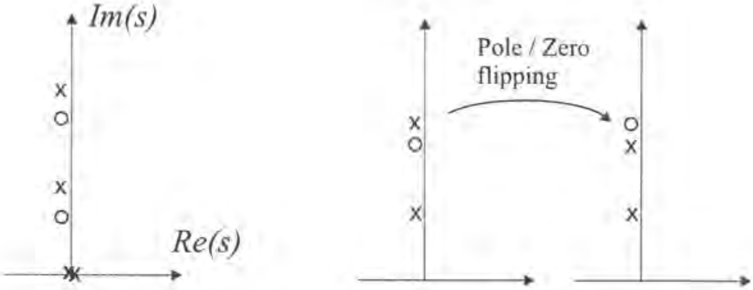

Figure 4.1: *(a) Alternating pole-zero pattern of a lightly damped flexible structure with collocated actuator and sensor. (b) Pole-zero flipping for a non-collocated system.*

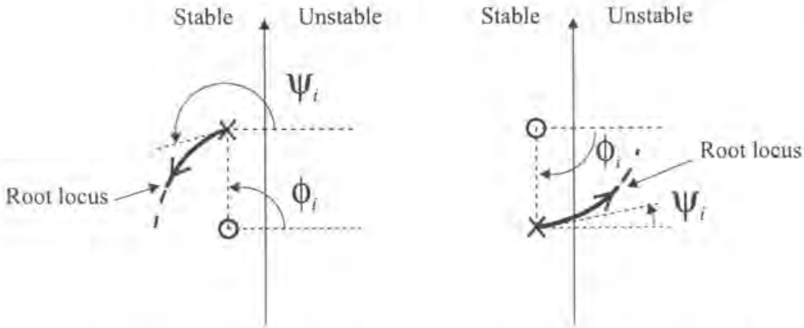

Figure 4.2: *Detail of a root locus showing the effect of the pole-zero flipping on the departure angle from a pole. Since the contribution of the far away poles and zeros is unchanged, that of the pole and the nearby zero, $\phi_i - \psi_i$ must also remain unchanged.*

use of collocated actuator/sensor pairs is recommended whenever it is possible.

This interlacing property of the poles and zeros no longer holds for a non-collocated control, and the root locus plot may experience severe alterations for small parameter changes. This is especially true when the sequence of poles and zeros along the imaginary axis is reversed as in Fig.4.1.b. This situation is called a *pole-zero flipping*. It is responsible for a phase uncertainty of 360^0, and the only protection against instability is provided by the *damping* (systems which are prone to such a huge phase uncertainty can only be *gain-stabilized*).

4.2 Pole-zero flipping

Recall that the root locus shows, in a graphical form, the evolution of the poles of the closed-loop system as a function of the scalar gain g applied to the compensator. The open-loop transfer function GH includes the structure, the compensator, and possibly the actuator and sensor dynamics, if necessary. The root locus is the locus of the solution s of the closed-loop characteristic equation $1 + gGH(s) = 0$ when the real parameter g goes from zero to infinity. If the open-loop transfer function is written

$$GH(s) = k\frac{\prod_{i=1}^{m}(s - z_i)}{\prod_{i=1}^{n}(s - p_i)} \tag{4.1}$$

the locus goes from the poles p_i (for $g = 0$) to the zeros z_i (as $g \to \infty$) of the open-loop system, and any point P on the locus is such that

$$\sum_{i=1}^{m} \phi_i - \sum_{i=1}^{n} \psi_i = 180^0 + l\,360^0 \tag{4.2}$$

where ϕ_i are the phase angles of the vectors $\vec{a_i}$ joining the zeros z_i to P and ψ_i are the phase angles of the vector $\vec{b_i}$ joining the poles p_i to P (see Fig.4.10). There are $n - m$ branches of the locus going asymptotically to infinity as g increases.

Consider the departure angle from a pole and the arrival angle at the zero when they experience a pole-zero flipping; since the contribution of the far away poles and zeros remains essentially unchanged, the difference $\phi_i - \psi_i$ must remain constant after flipping. As a result, a nice stabilizing loop before flipping is converted into a destabilizing one after flipping (Fig.4.2). If the system has some damping, the control system is still able to operate with a small gain after flipping.

Since the root locus technique does not distinguish between the system and the compensator, the pole-zero flipping may occur in two different ways:

- There are compensator zeros near system poles (this is called a *notch filter*). If the actual poles of the system are different from those assumed in the compensator design, the notch filter may become inefficient (if the pole moves away from the zero), or worse, a pole-zero flipping may occur. This is why notch filters have to be used with extreme care. As we shall see in later chapters, notch filters are generated by optimum feedback compensators and this may lead to serious robustness questions if the parameter uncertainty is large.

- Some actuator/sensor configurations may produce pole-zero flipping within the system alone, for small parameter changes. These situations are often associated with a pole-zero (near)cancellation due to a deficiency in the controllability or the observability of the system. In some cases, however, especially if the damping is extremely light, instability may occur. No pole-zero flipping can occur within the structure if the actuator and sensor are collocated.

The following sections provide examples illustrating these points.

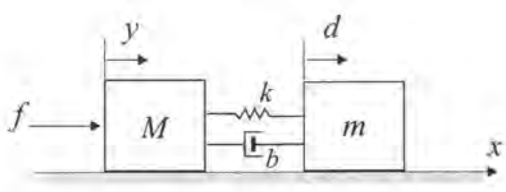

Figure 4.3: *Two-mass problem.*

4.3 Collocated control

Consider the two-mass problem of Fig.4.3. The system has a rigid body mode along the x axis; it is controlled by a force f applied to the main body M. A flexible appendage m is connected to the main body by a spring k and a damper b. In this section, a position control system will be designed, using a sensor placed on the main body (collocated); a sensor attached to the flexible appendage will be considered in the next section.

With f representing the control torque and y and d being the attitude angles, this problem is representative of the single-axis attitude control of a satellite, with M representing the main body, and the other inertia representing either a flexible appendage like a solar panel (in which case the sensor can be on the main body, i.e. collocated), or a scientific instrument like a telescope which must be accurately pointed towards a target (now the sensor has to be part of the secondary structure; i.e. non-collocated). A more elaborate single-axis model of a spacecraft is considered in Problem P.2.8.

The system equations are :

$$M\ddot{y} + (\dot{y} - \dot{d})b + (y - d)k = f \tag{4.3}$$

$$m\ddot{d} + (\dot{d} - \dot{y})b + (d - y)k = 0 \tag{4.4}$$

With the notations

$$\omega_o^2 = k/m, \quad \mu = m/M, \quad 2\xi\omega_o = b/m \tag{4.5}$$

the transfer functions between the input force f and y and d are respectively :

$$G_1(s) = \frac{Y(s)}{F(s)} = \frac{s^2 + 2\xi\omega_o s + \omega_o^2}{Ms^2\,[s^2 + (1+\mu)\,(2\xi\omega_o s + \omega_o^2)]} \tag{4.6}$$

$$G_2(s) = \frac{D(s)}{F(s)} = \frac{2\xi\omega_0 s + \omega_0^2}{Ms^2\,[s^2 + (1+\mu)\,(2\xi\omega_o s + \omega_o^2)]} \tag{4.7}$$

$$G_2(s) \simeq \frac{\omega_0^2}{Ms^2\,[s^2 + (1+\mu)\,(2\xi\omega_o s + \omega_o^2)]} \tag{4.8}$$

Approximation (4.8) recognizes the fact that, for low damping ($\xi \ll 1$), the far away zero will not influence the closed-loop response. There are two poles near the imaginary axis. In $G_1(s)$, which refers to the collocated sensor, there are two zeros also near the imaginary axis, at $(-\xi\omega_0 \pm j\omega_0)$. As observed earlier, these zeros are identical to the poles of the modified system where the main body has been blocked (i.e. constrained mode of the flexible appendage). When the mass ratio μ is small, the polynomials in the numerator and denominator are almost equal, and there is a pole-zero cancellation.

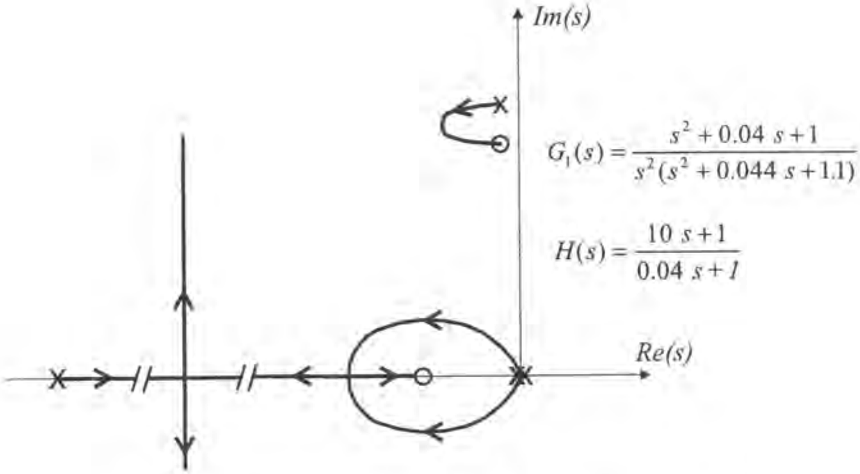

Figure 4.4: *Root locus plot for the collocated control.*

Let us consider a *lead compensator*

$$H(s) = g\frac{Ts + 1}{\alpha Ts + 1} \qquad (\alpha < 1) \tag{4.9}$$

It includes one pole and one zero located on the negative real axis; the pole is to the left of the zero. Figure 4.4 shows a typical root locus plot for the collocated case when $\omega_0 = 1$, $M = 1$, $\xi = 0.02$ and $\mu = 0.1$. The parameters of the compensator are $T = 10$ and $\alpha = 0.004$. Since there are two more poles than zeros ($n - m = 2$), the root locus has two asymptotes at $\pm 90^0$. One observes that the system is stable for every value of the gain, and that the bandwidth of the control system can be a substantial part of ω_0. The lead compensator *always* increases the damping of the flexible mode (see Problem P.4.5).

If there are not one, but several flexible modes, there are as many pole-zero pairs and the number of poles in excess of zeros remains the same ($n - m = 2$ in this case), so that the angles of the asymptotes remain $\pm 90^0$ and the root locus never leaves the stable region. The lead compensator increases the damping ratio of *all* the flexible modes, but especially those having their natural frequency between the pole and the zero of the compensator. Of course, we have assumed that the sensor and the actuator have perfect dynamics; if this is not the case, the foregoing conclusions may be considerably modified, especially for large gains.

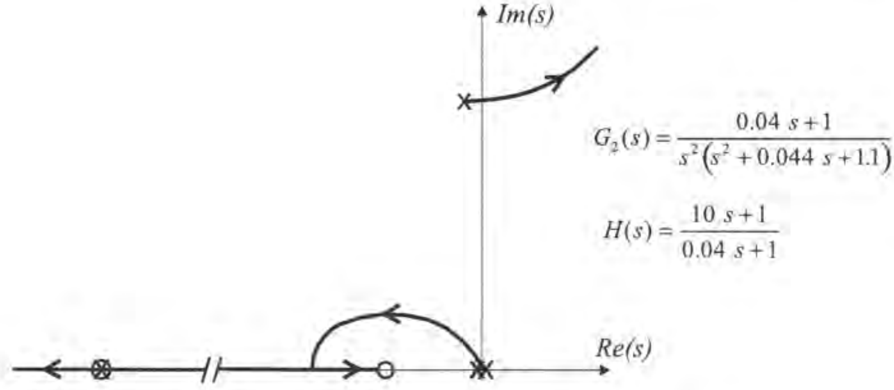

Figure 4.5: *Root locus of the lead compensator with non-collocated control.*

4.4 Non-collocated control

Figure 4.5 shows the root locus plot for the lead compensator applied to the non-collocated open-loop system characterized by the transfer function $G_2(s)$, Equ.(4.7), with the following numerical data: $\omega_0 = 1$, $M = 1$, $\mu = 0.1$, $\xi = 0.02$. The excess number of poles is in this case $n - m = 3$ so that, for large gains, the flexible modes are heading towards the asymptotes at $\pm 60^0$, in the right half plane. For a gain $g = 0.003$, the closed-loop poles are located at $-0.0136 \pm 0.0505j$ and $-0.0084 \pm 1.0467j$ (these locations are not shown in Fig.4.5 for clarity: the poles of the rigid body mode are close to the origin and those of the flexible mode are located between the open-loop poles and the imaginary axis). The corresponding Bode plots are shown in Fig.4.6; the phase and gain margins are indicated. One observes that even with this small bandwidth (crossover frequency $\omega_c = 0.056$), the gain margin is extremely small. A slightly lower value of the damping ratio would make the closed-loop system unstable (Problem P.4.1).

4.5 Notch filter

A classical way of alleviating the effect of the flexible modes in non-collocated control is to supplement the lead compensator with a notch filter with two zeros located near the flexible poles:

$$H(s) = g \cdot \frac{Ts+1}{\alpha Ts+1} \cdot \frac{s^2/\omega_1^2+1}{(s/a+1)^2} \tag{4.10}$$

The zeros of the notch filter, at $s = \pm j\omega_1$, are selected right below the flexible poles. The double pole at $-a$ aims at keeping the compensator proper (i.e. the